GEOQuébec 2015
Challenges from North to South
Des défis du Nord au Sud

Assessment of permafrost conditions in support of the rehabilitation and adaptation to climate change of the Iqaluit airport, Nunavut, Canada.

Valérie Mathon-Dufour, Michel Allard
Centre d'études nordiques, Université Laval, Québec, Québec, Canada
Anne-Marie LeBlanc
Geological Survey of Canada, Natural Resources Canada, Ontario, Canada

ABSTRACT
Iqaluit, the territorial capital of Nunavut and hub for air transport in the eastern Canadian Arctic, had an airport in poor condition and not adapted to the expected increase in air traffic in the coming years. In fact, the runway, taxiways and aprons are affected by permafrost degradation. This study aims to contribute to the development of an integrated geoscientific approach to make up for lack of adequate characterization of permafrost during construction in order to support rehabilitation work now in progress at the Iqaluit airport and adapt the infrastructures to new climatic conditions. The results confirm that the initial conditions (e.g. drainage, cryostratigraphy) of the terrain have a considerable impact on the current stability of the infrastructure. In addition, the presence of the infrastructure itself modify the surface conditions (e.g. albedo, drainage) which have an impact on the thermal regime of permafrost.

RÉSUMÉ
Iqaluit, capitale territoriale et plaque tournante du transport aérien dans l'est de l'Arctique canadien, possèdait jusqu'à récemment un aéroport en mauvais état et mal adapté à l'augmentation prévue du trafic aérien pour les prochaines années. En effet, la piste, les voies d'accès et le tarmac sont endommagés par divers processus de dégradation du pergélisol. La présente étude vise à contribuer à la mise au point d'une approche géoscientifique intégrée permettant de compenser l'absence de caractérisation adéquate du pergélisol lors de la construction dans le but d'appuyer les travaux de réfection nécessaires à l'aéroport d'Iqaluit et d'adapter les infrastructures aux nouvelles conditions climatiques. Les résultats obtenus confirment que les conditions initiales (p.ex. drainage, cryostratigraphie) du terrain ont un impact considérable sur la stabilité actuelle des infrastructures. De plus, la présence de l'infrastructure elle-même a pour effet de modifier les conditions de surface (p.ex. albédo, drainage) entraînant un ajustement du régime thermique du pergélisol à ces nouvelles conditions.

1 INTRODUCTION

The Iqaluit International Airport, in Nunavut, was built by the US Army during the WWII and expanded during the late 1960's (Eno, 2003). At that time, little was known about transportation infrastructures built on permafrost. Back then, the climate was relatively stable and colder. Currently, the runway, taxiways, aprons and buildings are damaged by permafrost degradation related to global warming (Figure 1) which is predicted to go on (ACIA, 2004). Despite the periodic maintenance of paved surfaces and buildings, permafrost at the airport site has never been the subject of a detailed study. The main objective of this study is to acquire data and knowledge on permafrost properties and processes affecting the performance of the infrastructure in order to compensate for the lack of existing information, to support the planned repairs, and adapt the infrastructure to new climatic conditions.

2 STUDY SITE

The city of Iqaluit (63°45'23"N, 68°33'21"W) is located southeast of Baffin Island in a valley open on Frobisher Bay, which is an inlet reaching out to the Hudson strait and the Arctic Ocean (Figure 2).

Figure 1: Differential settlement (left) and linear depression (right) caused by permafrost degradation at the Iqaluit Airport.

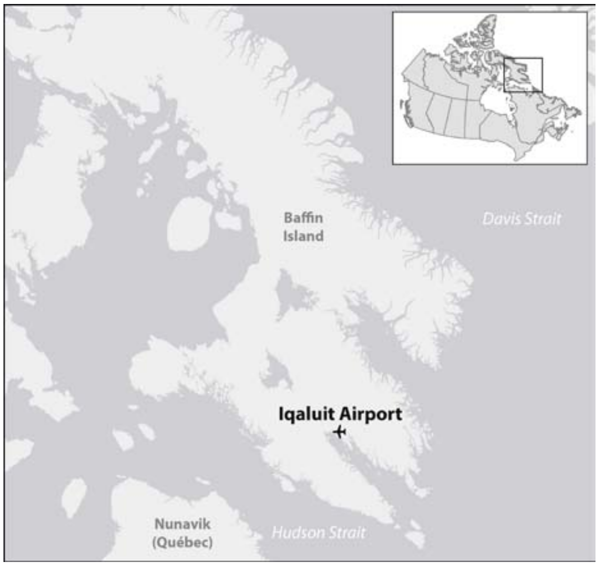

Figure 2: Location of the Iqaluit Airport, Nunavut.

The mean annual air temperature (MAAT) averages -8.9°C in Iqaluit throughout the period of 1951 to 2013. The minimum and maximum MAATs recorded for this period were respectively -12.4 and -4°C. The MAAT have slightly increased since the early fifties by 1.3°C (Figure 3). However, this increase did not happen steadily. The MAAT increased moderately from the 1950s until the end of the 1970s and then they abruptly increased since the 1990s, interrupted by a short period of cooling during the 1980s (Environment Canada, 2014).

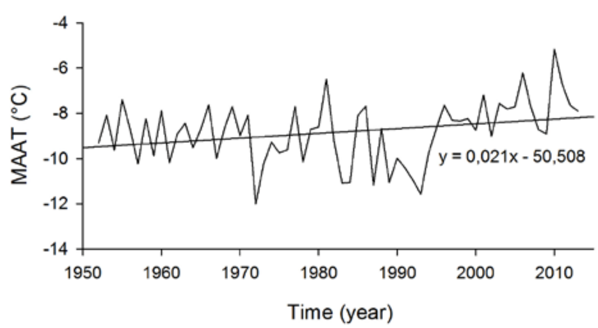

Figure 3: Mean annual air temperature (MAAT) at Iqaluit airport for the period of 1951 to 2013 (meteorological record from Environment Canada).

Surficial geology mapping was completed by Allard *et al.* (2012) (Figure 4). The soils consist of glaciofluvial (GFp and GFr), glaciomarine (GMd) and marine (Mn) sediments forming a rather flat sandur-delta of sand and gravel deposited during the retreat of the ice sheet and during marine transgression, around 7 ka ago. The sandur-delta surface is at an elevation of≈ 30 m which is the postglacial marine (washing) limit in the region. The runway is oriented along a southeast-northwest axis and is partly enclosed between Precambrian bedrock (R) hills with partial and uneven till cover (Tb and Tv), which have been partly blasted during extension works to clear the approach area. Lacustrine sediments (Lv) are found occasionally over the area and composed of clayey silts deposited in former lakes that have been drained to expand the infrastructures. Fluvial sediments (At and Ap) were deposited along the Sylvia Grinnell River and one smaller creek (Carney Creek) crossing the city during the incision of the outwash sediments.

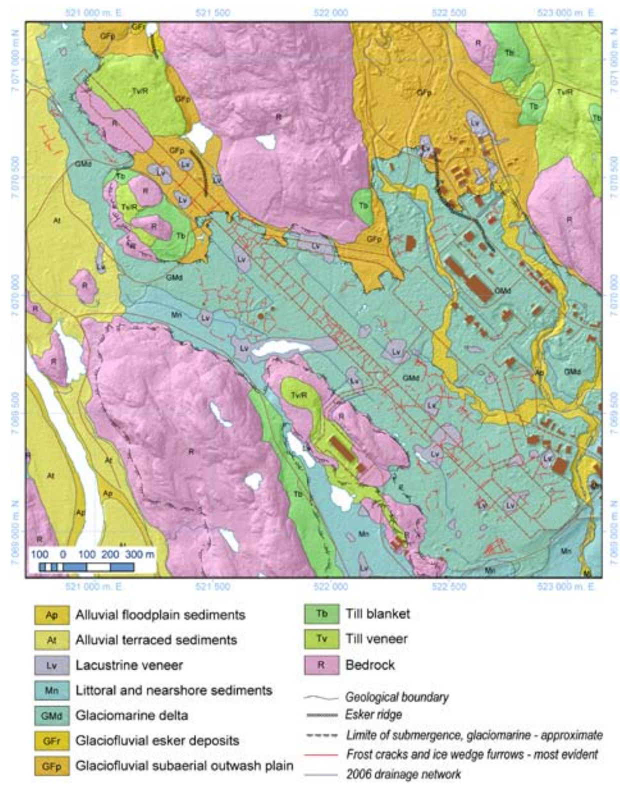

Figure 4: Surficial geology of the Iqaluit Airport area (modified from Allard *et al*., 2012).

3 METHODOLOGY

3.1 Multi-year photo-interpretation and historical analysis

Assessment of pre-construction and actual terrain conditions, such as drainage network and landforms indicative of the presence of ground ice (e.g. tundra polygons), were produced by interpreting aerial photographs dating back from the initial phases of construction (1948) to recent high-resolution satellite images (2008). In parallel, archived reports and other documents were searched to retrieve all possible relevant information about the airport history, such as expansion projects, permafrost related problems and repairs.

3.2 Permafrost drilling and coring

In total, 23 deep boreholes (between 8 and 15 m) and seven shallow boreholes (between 1.1 and 4.5 m) were drilled in the airport area (Figure 5). In the summer 2010 and 2011, 11 drill holes were made with an Air Track drill. Five sites were instrumented with thermistor cables. In order to better characterize the cryostatigraphy, a coring campaign took place in 2013. Twelve supplementary holes were cored with a diamond drill operating with drilling fluid cooled to ground temperature to extract intact permafrost cores. The frozen core samples were shipped to Université Laval for laboratory analyses. The drill type was a Versa Drill operated by a contractor. The core diameter is 83 mm (PQ3 size) and the average drill hole depth was 8 m.

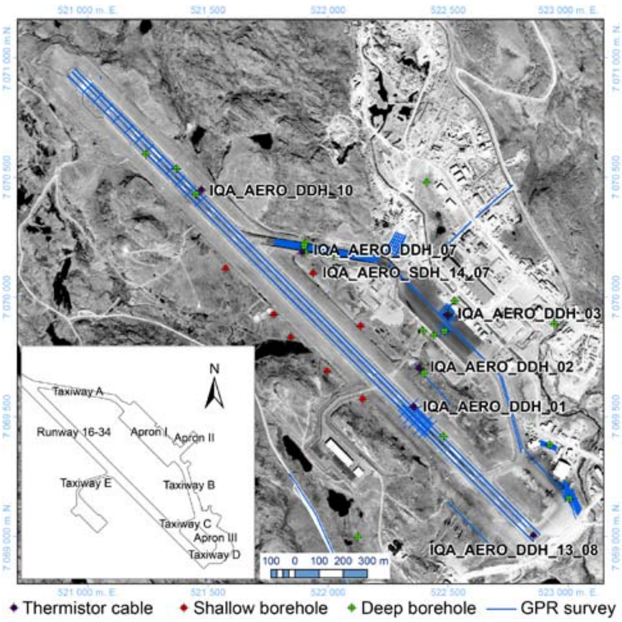

Figure 5: Location of boreholes, thermistor cable and GPR surveys.

3.3 Laboratory analysis

Frozen intact core samples were sent to the Institut National de la Recherche Scientifique Eau-Terre-Environnement (INRS-ETE) in order to make a three-dimensional image reconstruction using a CT-Scan (Siemens Somaton Sensation 64). Numerical image analysis allowed the characterization of air, soil and ice contents and cryostructure of the samples.

Conventional laboratory analyzes were performed on selected samples according to the sample management protocol of the Centre for Northern Studies (2013). These analyzes include calculation of water content, particle size distribution of coarse particles by sieving, removal of organic matter by loss on ignition, elimination of heavy minerals, deflocculation and particle size distribution of fine particles using a laser refractometer.

3.4 Ground temperature measurements and compilation from thermistor cables

Six thermistor cables were installed in drill holes (Table 1). The first one (IQA_DDH_02) was set in a drill hole in natural terrain between the runway and the apron in summer 2010. Four more cables were set in drill holes in summer 2011: IQA_AERO_DDH_01 in the runway, IQA_AERO_DDH_03 in a linear settlement in the Apron I, IQA_AERO_DDH_07 in the shoulder of taxiway A, and IQA_AERO_DDH_10 in the shoulder of the runway along the northern section. A final cable was installed in a drill hole in the pavement at the runway threshold 35, in 2013 (IQA_AERO_DDH_13_08).

At each site, a thermistor (model YSI-44033) string was inserted in PVC tubing, filled with silicone oil and placed in the drill hole, and connected to a data logger (model XR-420 from RBR Inc.). Some data loggers were placed 1m below ground level for security reasons. In these cases, a second data logger (model EM-50 from Decagon Inc.) was installed in a service hole to allow the recording of temperatures close to the surface.

Table 1: Thermistor cable, surface conditions and depth of the deepest thermistor.

Cable identification	Surface	Depth (m)
IQA_DDH_02	Sand and gravel w/ sparse vegetation	15
IQA_AERO_DDH_01	Pavement - Runway	14.25
IQA_AERO_DDH_03	Pavement – Apron I	10
IQA_AERO_DDH_07	Sand and gravel - Shoulder	15
IQA_AERO_DDH_10	Sand and gravel - Shoulder	15
IQA_AERO_DDH_13_08	Pavement - Runway	8

3.5 Ground penetrating radar surveys

Ground Penetrating Radar (GPR) (PulseEkko 100® by Sensors and Software) was used to locate cryostratigraphic units and reflectors in the embankments and surficial deposits. Survey lines were run at the 50, 100 and 200 MHz frequencies over various sectors of the airport such as the runway, taxiways, aprons and natural terrain (Figure 5). The surveys were made in the reflection mode. GPR surveys of the runway have been synthesized in a composite interpreted profile combining the three frequencies.

The signal speed was determined using the hyperbolic reflector method integrated in the Ekko_View Deluxe software (Sensor and Software Inc., 2003). For surveys carried out on paved surfaces, the average signal speed used was 0.11 m/ns. This average speed coincides with the value obtained using the common midpoint method (CMP) conducted in 2010 by LeBlanc et al. (2012).

4 RESULTS

4.1 Observations on permafrost related problems

Data integration of multi-year photo-interpretation, historical document analysis and on-site observation allowed to determine the main problems affecting the Iqaluit airport. The key issues are frost cracking processes, linear depressions associated with ice wedges, differential settlements and sinkholes.

Areas affected by frost cracking processes cover the entire airport. These cracks are caused, by the thermal contraction of the ground during rapid drops in temperature during winter. In the pavement, they are usually superficial and follow the tensile stress pattern which is at right angles to the infrastructure. However, some of them follow the cracking pattern associated with the underlying preconstruction ice wedge network (Figure 4). This pattern is larger in size, extends in the natural terrain, and is not consistent with the tensile stress pattern. These frost cracks may, in thin embankment areas, occur with linear depressions that are associated with the degradation of the upper part of ice wedges near the permafrost table. Most of the sectors affected by important differential settlements and instabilities spatially coincide with the original streams and lakes network that was filled to increase the size of the runway, taxiways and aprons. Drilling in those areas confirmed the presence of massive ice and ice-rich fine-grained sediments (Figure 6).

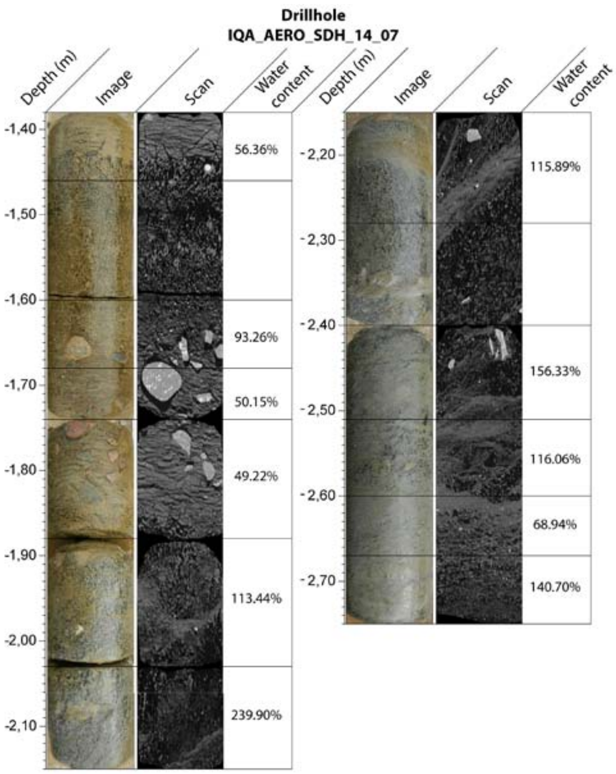

Figure 6: Cores, images of scanned samples and water content between -1.38 to -2.75 m depth at drill site IQA_AERO_SDH_14_07 near the taxiway-A.

4.2 Cryostratigraphy

Different sedimentary environments were observed at the airport (Figure 7). The surficial geology is composed mostly of sandy and gravelly sediments where abundant pore ice is found. In the proximal part of the sandur-delta, coarse glaciofluvial sediments are over 6 m thick and they are overlaying a thin layer of sandy or clayey marine sediments. In the distal part of the delta, the coarse surficial layer seems to get generally thinner (about 3 m) and overlies very ice-rich stratified silt and sand layers of glaciomarine origin (foreset and bottom set beds) dominated by interstitial ice and segregation ice lenses. Fine ice-rich sediments of lacustrine origin are also found in patches of a few centimeters to more than 2 meters in thickness where pre-existing lakes were drained for the construction of the infrastructure. As well, coarse sediments without a fine matrix of alluvial origin were found where former streams were filled for the extension of the runway, aprons and taxiways.

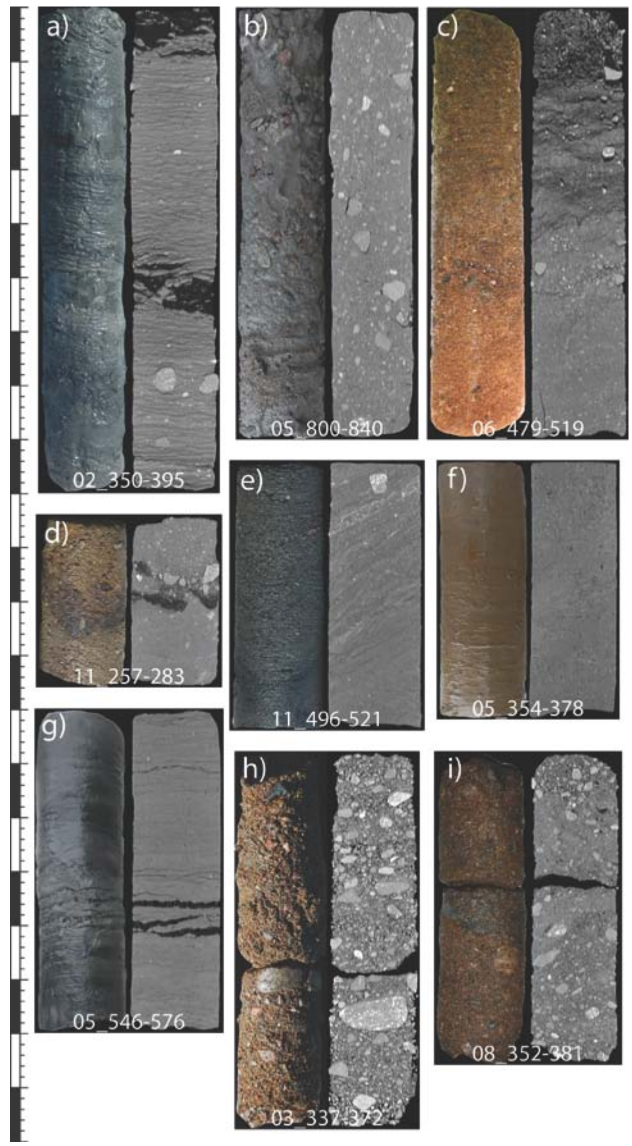

Figure 7: Representative samples and scan images of different sedimentary environments at the airport: a) Lacustrine (L) clayey silt, b) Till (T), c) Glaciofluvial (GFp) sand and gravel, d) Preconstruction organic layer (O), e) Glaciomarine (GMd) silty sand from foreset beds, f) Nearshore (GMn) fine sand, g) Glaciomarine (GMd) clayey silt from bottom set beds, h) Alluvial (Ap) sand and gravel without fines, i) Glaciomarine (Gmd) sand and gravel from top set beds.

The preconstruction active layer/permafrost contact could be observed in the cores drilled through the infrastructure foundation. The former soil surface and active layer sequence is composed of an ice-rich organic horizon underlain by a cryoturbated soil layer and an ice-rich layer (transient layer) containing aggradation ice corresponding to the top of the paleo-permafrost table. Two large ice wedges were cored through and show typical vertically oriented vein structures with sediments inclusions. Dates of 7.2 to 7.4 ka on marine shells found in the frozen glaciomarine sediments correspond with known deglaciation time in Iqaluit (Blake, 1966; Matthews, 1967). Dates on organic matter of 12-18 ka, indicate the incorporation of glacially eroded old carbon in marine sediments at deglaciation time.

4.3 Ground thermal regime

Thermal profiles of sites located under paved surfaces show generally warmer temperatures than those located in the shoulder and the natural terrain (Figure 8). During the thaw season, sites located under paved surfaces show that the heat wave progresses faster, deeper and over a longer period of time, than those located in the shoulder and natural ground (Figure 9). Temperature data from the active layer shows that the thawing period is 16 to 27 days longer for sites under paved surfaces than under natural terrain and shoulder embankments. In addition, the thawing of the active layer for sites under paved surfaces occurs earlier than at the other sites, even before the air temperature rises above 0°C. Compared to naturel ground, active layer thickness is up to 1.47 m more for sites under paved surfaces and 0.89 m more under embankments in early September 2014 (Table 2).

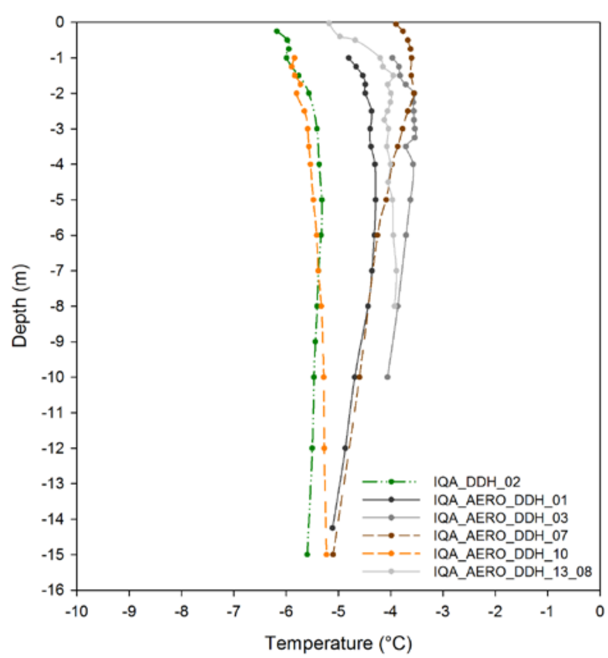

Figure 8: Mean annual temperature profiles at thermistor cable sites for the climatic year of 2013.

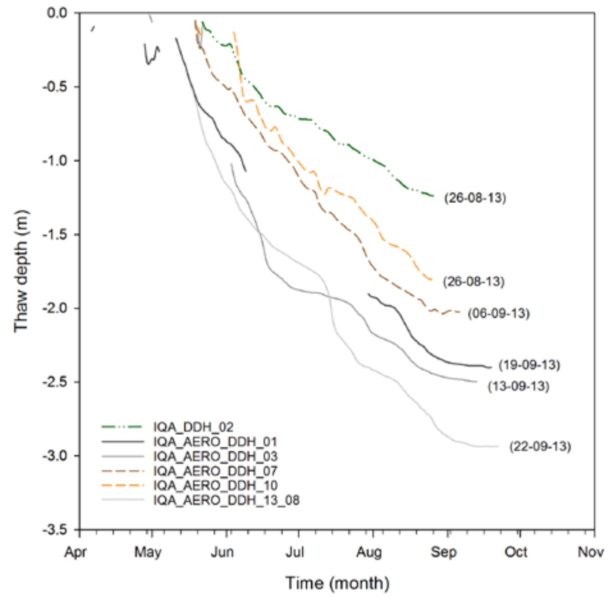

Figure 9: Thaw front advance during the thawing season and date of the maximum of the active layer thickness for each site in 2013.

Ground temperatures of sites IQA_AERO_DDH_03 and IQA_AERO_DDH_07 show a time interval between the fall of the surface soil layers and permafrost table below 0°C and the complete freezing of the active layer. The delay lasted more than 110 days for site IQA_AERO_DDH_03, in 2011 and a mean of about 50 days at site IQA_AERO_DDH_07, which indicate high water content within the active layer. Both sites also show a longer zero curtain period, during which ground temperatures stay near 0°C delaying the complete freezing of the active layer. This interval is caused by the latent heat released at the freezing front during the phase change of water (Table 3) (Harris *et al.*, 1988).

Table 2: Active-layer thickness at thermistor cable sites.

Sites	2010	2011	2012	2013	2014*
IQA_DDH_02	1.50	1.35	1.36	1.24	1.28
IQA_AERO_DDH_01	-	2.49	2.47	2.40	2.66
IQA_AERO_DDH_03	-	2.66	2.55	2.50	2.38
IQA_AERO_DDH_07	-	2.13	2.17	2.04	2.17
IQA_AERO_DDH_10	-	1.78	1.78	1.81	1.70
IQA_AERO_DDH_13_08	-	-	-	2.94	2.75

* As of September 2, 2014.

Table 3: Duration of active layer freezeback (period which extends between from the onset of the freezing at the permafrost table until the complete freezeback of the active layer) for the years 2010-2013.

Sites	2010	2011	2012	2013
IQA_DDH_02	58	33	30	31
IQA_AERO_DDH_01	-	21	22	44
IQA_AERO_DDH_03	-	110*	40	61
IQA_AERO_DDH_07	-	52	52	49
IQA_AERO_DDH_10	-	15	31	58
IQA_AERO_DDH_13_08	-	-	-	40

* minimal number of days

4.4 Ground penetrating radar composite profile of runway 16-34

The interpretation of GPR surveys helped to spatially interpolate the information obtained through drilling. This information includes geological contacts, thickness of active layer and embankments, location of the ice bodies and punctual objects such as ducts and wires (Judge et al., 2001; Moorman et al., 2003; Jørgensen and Andreasen, 2006). The multi-year photo-interpretation and the historical analysis including archived documentation also helped to produce the composite profile of the runway (Figure 10).

The embankment varies in thickness from a few centimeters to more than 3 m. Two sections were built on cuts in the original terrain: the northern section (between 2100 and 2700 m) on bedrock that was blasted during the late 1950s and the southern section of the runway (between 250 and 850 m) where 0.30 to 0.60 m of the soil surface were removed in the original levelling in 1941-42. The embankment of the old section was partly made of sand and gravel coming from the surficial material from the active layer of both sides of the runway. The embankment of the extension was made of blocky material obtained from blasting the bedrock hillside along the runway. During the same period, 0.30 to 1.70 m of material was added on top of the original pavement which was then paved again to raise the level of the runway. The current pavement thickness varies between 0.15 to 0.30 m. The stratigraphic contact between this fill material and the natural terrain beneath appears on the radar profiles, particularly along stretches where the original vegetation and organic cover was left in place. This contact could actually be visualized in drill holes IQA_AERO_DDH_13_06, 08 and 09 where the original terrain surface is now buried at -3.2, -2.7 and -2.2 m respectively.

The thaw front corresponds to thaw depth on the day of the survey, 5 August 2010. It was expressed by a strong planar reflector between 2.5 and 3.0 m. The thickness of the active layer was also validated at 2.75 m from the temperature record (depth of the 0 ℃ isotherm) at thermistor cable IQA_AERO_DDH_01. The reflector could not be followed in the bedrock under the northern end of the runway because there is practically no contrast in dielectric properties between frozen and thawed bedrock (LeBlanc et al., 2012).

Frost cracks crossed over during the GPR survey were geolocated. In many instances, they were underscored by a series of hyperbolic reflectors which are the typical signature of ice wedges (Fortier, 2004). The top of many ice wedges coincides with the base of the active layer (or top of permafrost), both in the natural terrain and under the runway. Wedge ice was cored from 3.3 to 5.65 m at borehole IQA_AERO_DDH_13_09 located in a linear depression, next to a major frost crack. Furthermore, some inactive (non-cracking and non-growing) ice wedges also occur at the pre-construction permafrost table under the foundation.

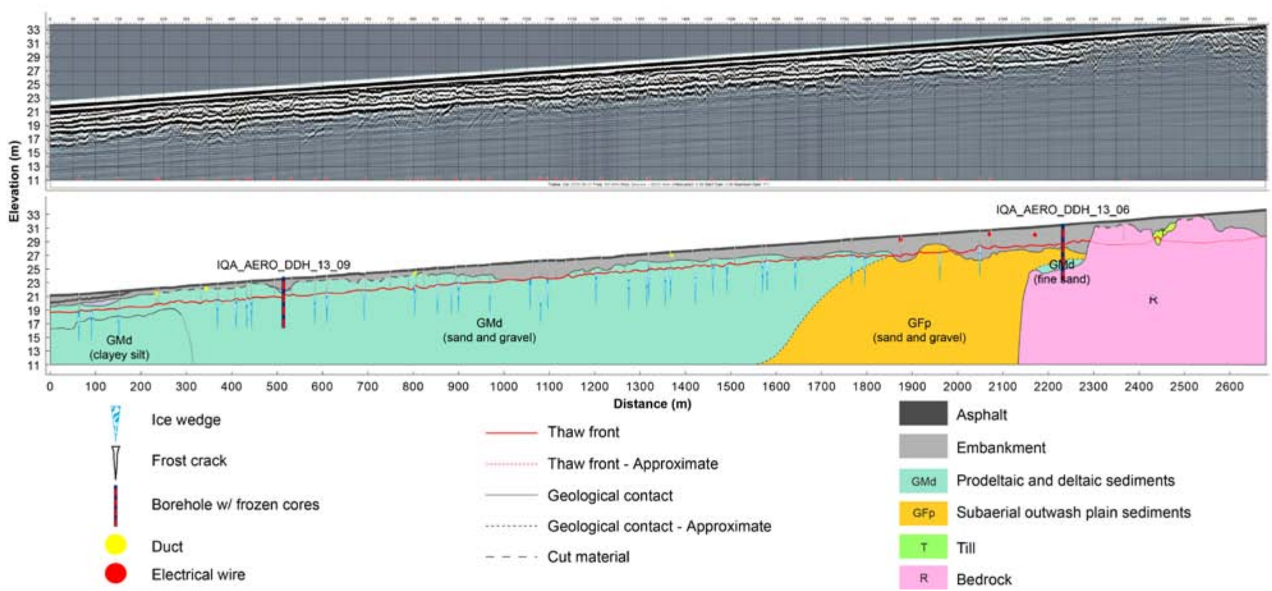

Figure 10: 100 MHz GPR profile and composite profile of the center line of the runway surveyed in August 2010.

5 DISCUSSION

5.1 Ground ice, ice-wedges and pavement frost cracking.

The drilling of cores reveals that the ground is generally ice-rich just below the active layer base or permafrost table. Should the climate continues to warm, thaw settlement will continue in conjunction with loss of bearing capacity (Andersland et Ladanyi, 1994). Some areas of the facility have rather high ice contents nearer to the surface; this is the case of the southern end of the runway and the area of the current terminal, the taxiway-A and apron-III. Indeed, the surface of the apron is already uneven due to differential settlements over the recent decade. In that area, icy soil layers start about 1.8 m deep, only a few centimeters below the current maximum thaw depth.

In addition, the extensive network of ice wedges extends practically everywhere under the runway, taxiways, aprons and aircraft parking areas. Only the northern section of the runway beyond taxiway-A has a smaller number of ice wedges near the surface because they were either buried under a thick blocky fill of 2-3 m in thickness or the runway was built directly over bedrock. GPR profiles show that many major cracks in the runway occur over ice wedges that were existent before construction. Their recent thawing under a warming climate since the mid-1990s is responsible for a number of linear settlements now affecting the pavement in areas of thin embankment. As the ice wedges are made of pure ice, their melting involves an increase in water content and loss of bearing capacity in adjacent soils. In addition, ice wedges are susceptible to suffosion and thermal erosion if water comes to flow to their contact (Fortier et al., 2007). Historical records relate this kind of events during early construction phases at the airport (Eno, 2003). The winter climate conditions are conducive to thermal contraction which maintains frost cracking active over the wedges. Open cracks at springtime allow for the percolation of water, causing the accumulation of water within the active layer.

5.2 Pre-construction and present drainage network

Some of the sectors where pre-existing creeks were filled and covered for the expansion of the apron and the runway are still impacted by the presence of ground water. The reoccurring settlement area that crosses the apron-I concentrates water in the active layer, which is deeper than in the surrounding terrain. The longer freezeback period in early winter, the absence of fine matrix in the active layer and the warmest temperature profile measured at the airport reveal the occurrence of high water content within the active layer.

The northern part of the runway, built over thick blocky material is affected by sinkholes that were mapped on the shoulders, some of them to the very edge of the pavement. It is probable that some cavities or loose embankment sections also exist under the thick pavement (0.30 m) in that sector of the runway due to water infiltration and erosion of fine particles through numerous frost cracks and former creeks that were filled during expansion works. The looseness of the fill material was observed as hole walls were not stable and some blocks collapsed during drilling operations in the northern section of the runway.

The faster rate of thaw front penetration and the deeper active layer under paved surfaces, and particularly the runway, is a probable cause for water retention of a perched water table over the permafrost observed during drilling operations. This can have an impact on the water (and ice) content of the active layer which combine with the lower albedo of the pavement, leads to an increase in ground temperature.

The impact of the former drainage network on the infrastructure instabilities can also be indicated by the presence of frost susceptible sediments deposited in former water bodies and within the current active layer. These sediments are very sensitive to freeze-thaw cycles and cause the formation of ice lenses responsible for frost heave and subsidence and a loss of bearing capacities during the thawing season around the junction of the runway and taxiway-A.

6 CONCLUSIONS

The results obtained in this study show that the initial terrain conditions prevailing before the airport construction, such as surficial geology, ground ice and the drainage network, have an important impact on the stability and the behavior of the infrastructure. In addition, the presence of the infrastructure itself, combined with the global warming has an effect on surface conditions, such as surface albedo and drainage network modifications. This leads to an adjustment of the permafrost thermal regime to these new conditions. As a result, thermal profiles located under asphalt pavement show warmer thermal profiles and a faster, deeper and longer thaw penetration than sites in the shoulders and the natural terrain, causing the pooling of water in the active layer under paved surfaces. In turn, water accumulated within the active layer causes a positive feedback loop and accelerates the ongoing process.

In the present context of accelerated global warming, the development of a new adaptation strategy is crucial. Currently, the facility is undergoing upgrades and updates to face the increase in air temperatures and the growing need in air transportation for the next 40 years. The newly acquired knowledge on the Iqaluit airport permafrost is considered in decision making, risk analyses and choices of engineering designs for repairs, resurfacing and expansions in order to have a modern infrastructure that shall be better adapted to the impacts of climate warming.

The next actions to be implemented in order to better understand the observed problems will include 1) the monitoring of the permafrost thermal regime, 2) one-dimensional numerical simulations of permafrost thermal regime, and 3) the collection and integration of geolocated data on problematic areas integrated into a permanent GIS.

ACKNOWLEDGEMENTS

The authors express their thanks to the Government of Nunavut and to Transport Canada for the opportunity awarded to carry research on permafrost properties and dynamics in such an interesting context of applied science as the Iqaluit airport. We also acknowledge the contribution of team members from Centre d'études nordiques and collaborators from Natural Resources Canada.

REFERENCES

ACIA, 2004. Arctic Climate Impact Assessment. Cambridge University Press, Cambridge, UK. 140 p.

Andersland, O. B., and Ladanyi, B. 1994. *An introduction to frozen ground engineering*. Chapman & Hall, Ltd., New York, N.Y. 384 p.

Allard, M., Doyon, J., Mathon-Dufour, V., LeBlanc, A.-M., L'Hérault, E., Mate, D., Oldenborger, G.A., & Sladen, W.E. 2012. Surficial geology, Iqaluit, Nunavut; Geological Survey of Canada, Canadian Geoscience Map 64 (preliminary version), scale 1:15 000. doi:10.4095/289503.

Blake Jr, W. 1966. End moraines and deglaciation chronology in northern Canada with special reference to southern Baffin Island. Geological Survey of Canada: Department of mines and technical surveys. Paper 66-26.

Eno, R.V. 2003. Crystal Two: the origin of Iqaluit. Arctic, 56: 63-75.

Environment Canada. 2014. The climate normals of Canada 1981-2010. http://www.climate.weatheroffice.gc.ca/climate_normals/stnselect_e.html. Accessed December, 2014.

Fortier, D. & Allard, M. 2004. Late Holocene syngenetic ice-wedge polygons development, Bylot Island, Canadian Arctic, Archipelago. Canadian Journal of Earth Sciences, 41: 997–1012.

Harris, S. A., French, H. M., Heginbottom, J. A., Johnston, G. H., Ladanyi, G. H., Sego, D. C., & Van Everdingen, R. O. 1988. La terminologie de pergélisol et notions connexes.

Jørgensen, A. S., & Andreasen, F. 2007. Mapping of permafrost surface using ground-penetrating radar at Kangerlussuaq Airport, western Greenland. Cold regions science and technology, 48(1): 64-72.

Judge, A. S., Tucker, C. M., Pilon, J. A., & Moorman, B. J. 1991. Remote sensing of permafrost by ground-penetrating radar at two airports in Arctic Canada. Arctic, 40-48.

Matthews, B. 1967. Late quaternary marine fossils from frobisher bay (Baffin Island, NWT, Canada). *Palaeogeography, Palaeoclimatology, Palaeoecology*, 3: 243-263.

Moorman, B. J., Robinson, S. D., & Burgess, M. M. (2003). Imaging periglacial conditions with ground-penetrating radar. Permafrost and Periglacial Processes, 14(4): 319-329.

LeBlanc, A. M., Mathon-Dufour, V., Allard, M., Oldenborger, G. A., Short, N., L'Hérault, E., & Sladen, W. E. 2012. Permafrost characterization at the Iqaluit International Airport, Nunavut, in support of decision-making and planning. Canada-Nunavut Geoscience Office. Summary of Activities, 2013, 131-142.

Centre d'études nordiques. 2013. Analyses géotechniques appliquées aux régions froides. Version 1.1. Unpublished. 26 p.